Available online at www.sciencedirect.com
SCIENCE DIRECT®
Journal of Crystal Growth 254 (2003) 80–85
JOURNAL OF CRYSTAL GROWTH
www.elsevier.com/locate/jcrysgro

Structure and photoluminescence of Mn-passivated nanocrystalline ZnO thin films

X.T. Zhang[a,b], Y.C. Liu[b,c,*], J.Y. Zhang[b], Y.M. Lu[b], D.Z. Shen[b], X.W. Fan[b], X.G. Kong[b]

[a] *Department of Physics, Harbin Normal University, Harbin 150080, People's Republic of China*
[b] *Key Laboratory of Excited State Processes, Changchun Institute of Optics, Fine Mechanics and Physics, Chinese Academy of Sciences, 16-East South Lake Road, Changchun 130021, People's Republic of China*
[c] *Advanced Center for Optoelectronic Functional Material Research, Northeast Normal University, Changchun 130024, People's Republic of China*

Received 9 July 2002; accepted 6 March 2003
Communicated by R. James

Abstract

We have studied the structure and the photoluminescence of Mn-passivated nanocrystalline ZnO thin films. The ZnO thin films were prepared by thermally oxidizing ZnS:Mn films grown by low-pressure metalorganic chemical vapor deposition. The structural properties of the ZnO films were examined by X-ray diffraction and X-ray photoelectron spectroscopy. It was demonstrated that the Mn passivation could dramatically change the emission characteristics of nanocrystalline ZnO thin films. The photoluminescence spectra of the films with an optimized Mn-doped concentration showed only ultraviolet emission, while the green emission was fully quenched due to the Mn passivation of the ZnO nanocrystallite surface. A core-shell structure model of the surface passivation is presented. The note of the oxygen vacancy (Vo**) as the dominant recombination center for green emission is discussed.
© 2003 Published by Elsevier Science B.V.

PACS: 78.55.Et; 81.07.Bc; 81.15.Gh; 76.30.Lh; 82.80.Pv

Keywords: A1. Crystal structure; A1. Photoluminescence; B1. Zinc compounds

1. Introduction

Wide-band gap ($E_g = 3.37\,\text{eV}$) ZnO with a wurtzite crystal structure has been used in a wide range of device applications [1–3], because of its electrical, optical and piezoelectric properties. Recently, there has been an increasing interest in high-quality ZnO films in order to obtain ultraviolet light-emitting and laser devices. Compared with other wide-band gap materials, ZnO has a higher exciton binding energy of 60 meV [4], resulting in more efficient exciton emissions at room temperature. However, in order to obtain the efficiency of the exciton

*Corresponding author. Key Laboratory of Excited State Processes, Changchun Institute of Optics, Fine Mechanics and Physics, Chinese Academy of Sciences, 16-East South Lake Road, Changchun 130021, People's Republic of China. Fax: +86-431-5955378.
E-mail address: ycliu@nenu.edu.cn (Y.C. Liu).

0022-0248/03/$ - see front matter © 2003 Published by Elsevier Science B.V.
doi:10.1016/S0022-0248(03)01143-6

luminescence, better understanding of the luminescence mechanism has become a subject of current investigations on the laser properties of ZnO [5–7]. There are generally two luminescence bands in the photoluminescence (PL) spectra of ZnO thin films [8,9]. One is an ultraviolet (UV) emission band at near 390 nm, which is attributed to the direct recombination of photogenerated charge carriers. The other is a green emission band. The two emission processes are in competition with each other. To understand the origin of the green emission, various mechanisms have been proposed, including oxygen vacancies [10–12], interstitial oxygen [13,14], zinc vacancies and interstitial zinc [15], or even impurities Cu [16]. In recent years, oxygen vacancies have been assumed to be the most likely candidate for the recombination centers involved in the green luminescence of ZnO [17,18]. In particular, oxygen vacancy without electron is thought to be the probably recombination center for the green emission.

A luminescence characteristic of manganese may also be expected in Mn-doped ZnO. The radii of Zn^{2+} and Mn^{2+} ions (0.83 and 0.91 Å, respectively) are similar, and the four-fold coordination of zinc with respect to oxygen is also typical of Mn. Nevertheless, investigators have not succeeded in observing the luminescence of manganese in ZnO, but instead it was observed that Mn quenched the green luminescence in ZnO [19]. The reason for the quenching is unclear.

In this paper, X-ray diffraction (XRD), X-ray photoelectron spectroscopy (XPS), and electron paramagnetic resonance (EPR) spectroscopy measurements were employed to investigate the effect of introducing Mn on the structure and the photoluminescence (PL) of nanocrystalline ZnO:Mn thin films. The films were prepared by thermally oxidizing ZnS:Mn thin films deposited by low-pressure metalorganic chemical vapor deposition (LP-MOCVD). A core-shell structural model of Mn-passivated ZnO nanocrystallite is proposed with the help of oxygen vacancy (Vo**) without electron as the recombination center for green emission.

2. Experimental procedure

The sample preparation processes without doped-Mn have been reported in a previous publication [20]. In this experiment, the gas flow rate of tricarbonyl-methyl-cyclopentadienyl-Mn (TCM) was fixed at 26 ml/min, and the other preparation parameters were the same as those reported in Ref. [19]. The thickness of the deposited ZnS:Mn thin films was about 500 nm. After deposition, thermal oxidation of the films was carried out in an oxygen ambient at an annealing temperature of 800°C for 2 h.

To characterize the film structure, X-ray diffraction (XRD) spectra were measured using a D/max-rA X-ray diffraction spectrometer (Rigaku) with a Cu K_α line of 1.54 Å. The XRD result indicated that the ZnO:Mn thin films, which consist of nanocrystallites of about 29 nm in average size, possessed a polycrystalline hexagonal wurtzite structure. PL spectra were measured using a micro-laser Raman spectrometer in a back-scattering geometry configuration. A He–Cd laser operated at a wavelength of 325 nm was used as the excitation source for the PL measurements. XPS measurements were performed to investigate the composition and the chemical bonding configurations of the ZnO:Mn thin films. EPR measurements were used to confirm the location of Mn at or near the surface of the ZnO nanocrystallites.

3. Results and discussions

3.1. Structure of the ZnO:Mn thin films

Fig. 1 shows the XRD spectra of the ZnS:Mn thin films with different Mn-doped concentrations annealed at 800°C. For comparison, the XRD spectrum for a ZnS thin film without Mn-doped annealed at 800°C is shown in Fig. 1(a). The XRD patterns confirm that ZnS completely transforms into ZnO with a polycrystalline hexagonal wurtzite structure. In order to evaluate the mean grain size of the films, Scherrer's formula [21] is adopted. The mean grain size of the films is about 28.8 nm for all the samples. By comparing the X-ray diffraction pattern of the Mn doped samples

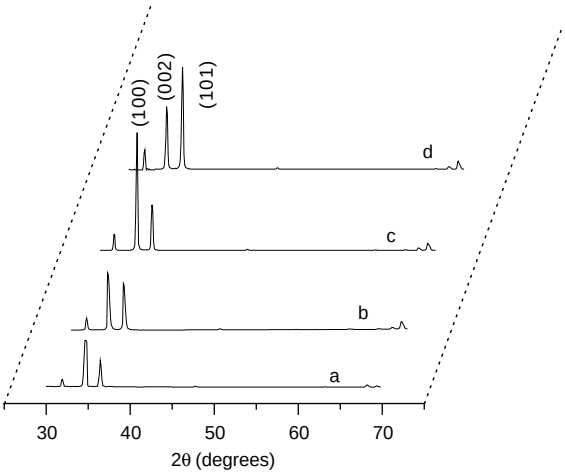

Fig. 1. XRD spectra for samples a–d (curve (a) without Mn; (b) flow rate of 26 ml/min; (c) flow rate of 106 ml/min; (d) flow rate of 160 ml/min).

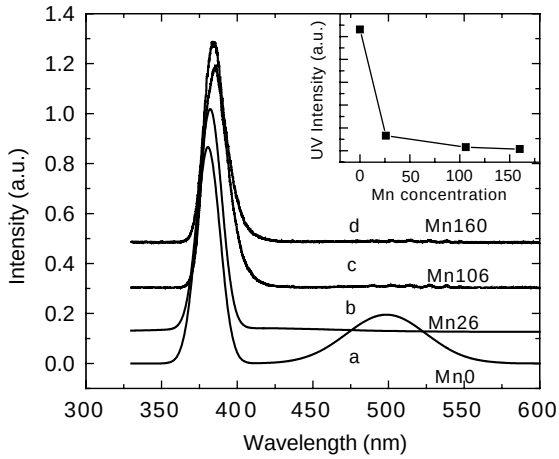

Fig. 2. Photoluminescence spectra for the samples, curve (a) sample a; (b) sample b; (c) sample c; (d) sample d, respectively. The inset represents the UV intensity as a function of Mn doping concentration.

(nano-ZnO:Mn) with that of the undoped sample (nano-ZnO), we see that no new peaks appear. The peak intensities and the crystal lattice constants change slightly. This indicates that the Mn concentration in the ZnO matrix is fairly dilute.

3.2. Photoluminescence of ZnO:Mn thin films

Fig. 2 shows the photoluminescence (PL) spectra of samples with different Mn-doped concentrations (nano-ZnO:Mn; b-26 ml/min, c-106 ml/min, d-160 ml/min) and sample a (nano-ZnO). Both ultraviolet and green emission bands, which have been well previously studied, are observed for sample a, as shown in Fig. 2(a). However, a single ultraviolet emission is observed without any visible emission for sample b with an optimized Mn-doped concentration. The inset in Fig. 2 shows the UV photoluminescence intensity as a function of Mn concentration. The photoluminescence intensity decreases with increasing Mn concentration. This is probably because the non-radiative recombination processes increase with increasing Mn. Note that the luminescence of manganese in ZnO is not observed in the PL spectrum of the ZnO:Mn films. As it is well known, only Mn^{2+} will substitute for Zn^{2+} in the ZnS lattice. In addition, the luminescence of Mn in ZnS can be observed [22]. Given the observed luminescence of Mn in ZnS, we deduce that Mn^{2+} does not substitute for Zn^{2+} in the ZnO lattice. Furthermore, after sample annealing, the impurities in the nanocrystallite will be redistributed to the surface of the nanocrystallite [22].

3.3. Mechanism of the green emission

To explain the above PL results, we will first discuss the mechanism behind the origin of the green photoluminescence band. It is generally thought that the green emission of ZnO originates from oxygen vacancies (Vo) [21,23–30]. Vanheusden et al. [18] suggested that the green emission of ZnO materials is due to the recombination of electrons in singly occupied oxygen vacancies with photo-excited holes in the valence band. Recently, first-principles theoretical results by Zhang et al. [31] supported this identification and showed that oxygen vacancies have a low formation enthalpy and are easily formed. The photogenerated electrons can be trapped by oxygen vacancies through a non-radiative decay, then they recombine with holes in the valence band. In addition, van Dijken et al. [32] proposed that the green emission is due

to the recombination of a shallowly trapped electron with a deeply trapped hole.

Here, the defect chemistry of ZnO is considered. ZnO has several types of defects such as interstitial atoms, vacancies and anionic and cationic impurities [33]. EPR studies show that oxygen vacancies with one electron (V*) are the dominant paramagnetic defect [9,17,18]. In macrocrystalline ZnO, these defects are represented as a level approximately 2 eV below the conduction band edge [33], and they are often assumed to be the recombination center responsible for the visible emission in ZnO. Previously, the green emission was identified as the recombination of an electron from the conduction band with the Vo* center. After capture of the addition electron the Vo (O^{2-}) center is electronically neutral. The neutral Vo center has an energy that is very close to the conduction band edge, and at room temperature almost all Vo centers are thermally dissociated into Vo* centers and conduction band electrons. The shift from 2 eV below the conduction band edge for the Vo* center to just below the conduction band edge for the neutral Vo center is due to the correlation energy of the two electrons in the oxygen vacancy [33]. Thus, the transition of an electron from the conduction band to a Vo* level can not produce photons with an energy of about 2 eV, as such a transition effectively take place between the conduction band edge and the Vo level. This means that the mechanism in which the Vo* is the recombination center for the green emission of ZnO is not correct. Recombination of an electron from the conduction band with a Vo** center can yield photons with an energy of about 2 eV. Such Vo** centers can be formed when a hole is trapped at a Vo* center. Hence, van Dijken et al. proposed the following the mechanism for the green emission [32]:

The photogenerated hole is trapped by surface states or defects (probably O^{2-}/O^{-}). The surface-trapped hole tunnels back into the nanocrystallite. Where it recombines with an electron to form the Vo** center [32]. Finally, the green emission is assigned to the recombination of a shallowly trapped electron with a deeply trapped hole in a Vo** center.

3.4. Core-shell structure of ZnO:Mn thin films

In order to study the composition and chemical bond configuration of ZnO:Mn films, we measure the XPS spectrum of ZnO nanocrystallites. Fig. 3 shows representative $Mn^{1/2}2p$ and O 1 s XPS spectra for sample a. One peak at about 641.5 eV for associated with the $Mn^{1/2}2p$ XPS spectrum is observed, as shown in Fig. 3(a). The peak is divided into two peaks with Gaussian-like shapes centered at 640.8 and 642.1 eV, indicating the co-presence of small amounts of Mn^{2+} and MnO_2 [34]. The O 1 s peak has a shoulder at the high-energy side, as shown in Fig. 3(b). The peak located at a low energy of about 530.02 eV (O1) corresponds to Zn-O bonding, while the higher energy peak located at about 531.51 eV (O2) corresponds to the OH group [35].

Fig. 4 shows the EPR spectrum for sample b. EPR spectra can be used to determine the location of Mn in the host material, since the hyperfine splitting of Mn is strongly dependent on its local environment. A six-line spectrum with symmetry sites is measured, as shown in Fig. 4(b). The lines are from the interaction with the ^{55}Mn nuclear spin ($I = 5/2$), indicating that Mn is embedded

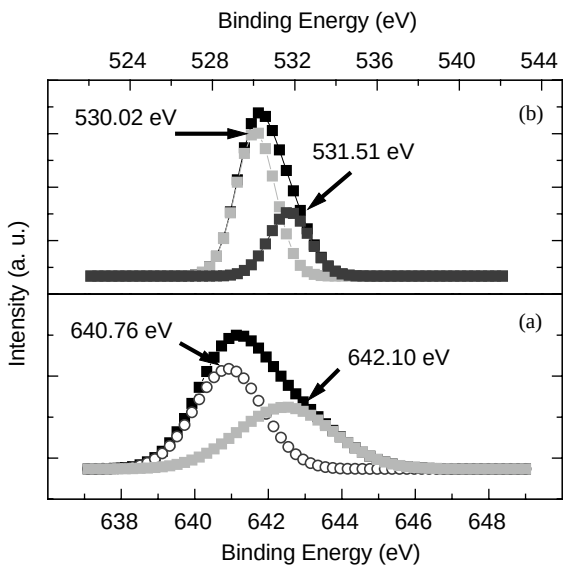

Fig. 3. XPS spectra calibrated by taking the carbon C 1 s peak (284.6 eV) as reference. (a) $Mn^{1/2}2p$ and (b) O1s.

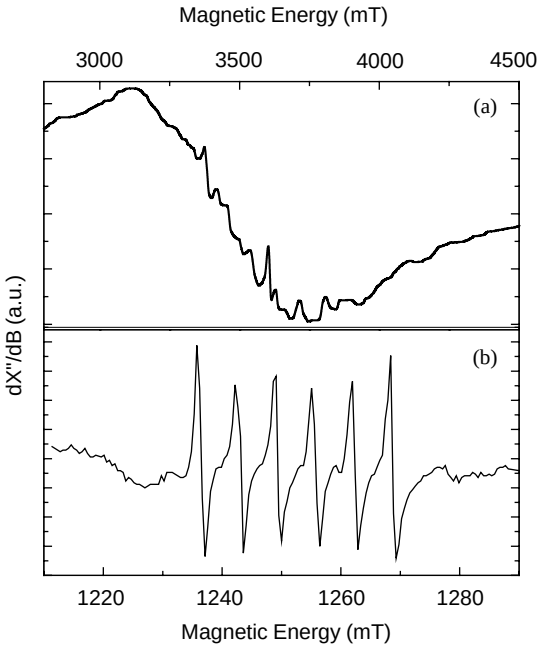

Fig. 4. (a) EPR spectrum taken at 9.5 GHz at room temperature, which shows a weak six-line spectrum superposed on a broad background. Despite its weakness, the six-line structure and $g = 2.003$ immediately identify ^{55}Mn in ZnO. (b) EPR spectrum of ZnS:Mn thin films.

inside the nanocrystal and substitutes for Zn in ZnS lattice (Ref. [22]). However, for ZnO:Mn we obtain a six-line spectrum with asymmetry sites, as shown in Fig. 4(a). Based on the asymmetric EPR spectrum and lack of observable luminescence of Mn in the films, we think that the majority of the Mn in ZnO:Mn is at or near the surface of the ZnO nanocrystallite. Together with the XPS and EPR results, a core-shell structure of Mn-passivated ZnO nanocrystallite is suggested, as shown in Fig. 5. The passivated ZnO nanocrystallite consists of three regions: the core, interfacial and MnO_2 regions. It is suggested that the interfacial layer is created by the OH group and Mn^{2+} ion [34]. Similar models have been presented for a MnO_2-passivated Si nanocrystallite system [34].

Because the passivated layer on the surface of the ZnO nanocrystallite has a potential energy large enough to prevent surface states from trapping photogenerated electrons or holes [33], the pathway to form the Vo** centers is blocked.

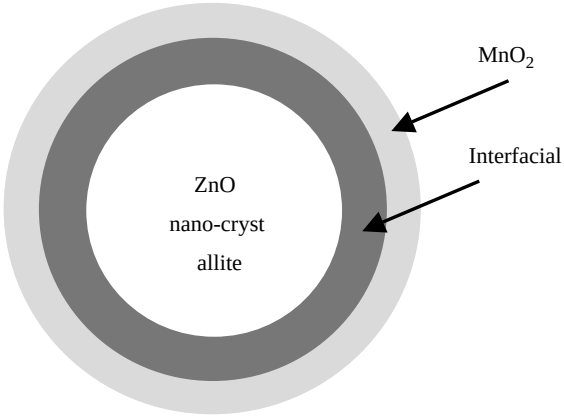

Fig. 5. A schematic core-shell structure of Mn-passivated ZnO nanocrystallite.

According to the mechanism of green emission and our model of a core-shell structure for ZnO:Mn films, a single ultraviolet emission from the nanocrystalline ZnO:Mn films is expected, while the green emission would be fully quenched, which agrees with the PL result.

4. Conclusion

A single UV emission at 3.25 eV is observed from the nanocrystalline ZnO:Mn thin films passivated by manganese. The green emission found in undoped ZnO is fully quenched by addition of Mn. We explain the observation of the single UV emission based on blocking of the formation of Vo** centers. A core-shell structure of Mn concentrated on the surface of ZnO nanocrystalline thin films is presented.

Acknowledgements

The authors thank Dr. J. Judy for her helpful discussions. This work was supported by the Program of CAS Hundred Talents, the National Natural Science Foundation of China (60176003), the Innovation Foundation of CIOMP, the Foundation of Excellent Researcher to go beyond Century of Ministry of Education of China, and Jilin Distinguished Young Scholar Program.

References

[1] J. Hu, R.G. Gordon, J. Electrochem. Soc. 139 (1992) 2014.
[2] A. Barkers, S. Crowther, D. Rees, Sensors Actuators A 58 (1997) 2291.
[3] F. Hamdani, D.J. Smith, H. Jang, W. Kim, A. Salvador, A.E. Botharev, J.M. Gibson, A.Y. Polyakov, M. Skowronski, H. Morkoc, J. Appl. Phys. 83 (1998) 983.
[4] K. Hümmer, Phys. Stat. Sol. 56 (1973) 249.
[5] N.W. Lawandy, R.M. Balachandran, A.S.L. Gomes, E. Sauvain, Nature 368 (1995) 436.
[6] H. Cao, J.Y. Xu, E.W. Seelig, R.P.H. Chang, Appl. Phys. Lett. 76 (2000) 2997.
[7] X.L. Wu, G.G. Siu, C.L. Fu, H.C. Ong, Appl. Phys. Lett. 78 (2001) 2285.
[8] S. Miyamoto, Jpn. J. Appl. Phys. 17 (1978) 1129.
[9] K. Vanheusden, C.H. Seager, W.L. Warren, D.R. Tallant, J.A. Voigt, Appl. Phys. Lett. 68 (1996) 403.
[10] N. Riehl, O. Ortman, Z. Elektrochem. 60 (1952) 149; P.H. Kasai, Phys. Rev. 130 (1963) 989.
[11] E.A. Kröger, H.J. Vink, J. Chem. Phys. 22 (1954) 250.
[12] I.Y. Prosanov, A.A. Politov, Inorg. Mater. 31 (1995) 663.
[13] D. Hahn, R. Nink, Phys.: Condens. Mater. 3 (1965) 311.
[14] M. Liu, A.H. Kitai, P. Mascher, J. Lumin. 54 (1992) 35.
[15] E.G. Bylander, J. Appl. Phys. 49 (1978) 1188.
[16] R. Dingle, Phys. Rev. Lett. 23 (1969) 579.
[17] M. Anpo, Y. Kubokawa, J. Phys. Chem. 88 (1984) 5556.
[18] K. Vanheusden, W.L. Warren, C.H. Seager, D.R. Tallant, J.A. Voigt, B.E. Gnade, J. Appl. Phys. 79 (1996) 7983.
[19] M. Liu, A.H. Kitai, P. Mascher, J. Lumin. 54 (1992) 35.
[20] X.T. Zhang, Y.C. Liu, Z.Z. Zhi, J.Y. Zhang, Y.M. Lu, D.Z. Shen, W. Xu, G.Z. Zhong, X.W. Fan, X.G. Kong, J. Phys. D 34 (2001) 3430.
[21] C.M. Mo, Y.H. Li, Y.S. Lin, Y. Zhang, L.P. Zhang, J. Appl. Phys. 83 (1998) 4389.
[22] D.J. Norris, N. Yao, F.T. Charnock, T.A. Kennedy, Nanoletters 1 (2001) 3.
[23] K. Borgohain, S. Mahamuni, Semicond. Sci. Technol. 13 (1998) 1154.
[24] S. Mahamuni, K. Borgohain, B.S. Bendre, V.J. Leppert, S.H. Risbud, J. Appl. Phys. 85 (1999) 2861.
[25] E.M. Wong, P.C. Searcon, Appl. Phys. Lett. 74 (1999) 2939.
[26] L. Guo, S.H. Yang, C.L. Yang, P. Yu, J.N. Wang, W.K. Ge, G.K.L. Wang, Appl. Phys. Lett. 76 (2000) 2901.
[27] S.A. Studenikin, N. Golego, M. Cocivera, J. Appl. Phys. 84 (1998) 2287.
[28] M. Haase, H. Weller, A. Henglein, J. Phys. Chem. 92 (1988) 482.
[29] L. Spanhel, M.A. Anderson, J. Am. Chem. Soc. 113 (1991) 2826.
[30] L. Guo, S.H. Yang, C.L. Yang, P. Yu, J.N. Wang, W.K. Ge, G.K.L. Wang, Chem. Mater. 12 (2000) 2268.
[31] S.B. Zhang, S.H. Wei, A. Zunger, Phys. Rev. B 63 (2001) 75205.
[32] A. Van Dijken, E.A. Meulenkamp, D. Vanmaekelbergh, A. Meijerink, J. Phys. Chem. B 104 (2000) 1715.
[33] E.A. Kröger, The Chemistry of Imperfect Crystals, North-Holland, Amsterdam, 1964, p. 691.
[34] Q.W. Chen, D.L. Zhu, Y.H. Zhang, Appl. Phys. Lett. 77 (2000) 854.
[35] L.J. Meng, C.P. Moreira, M.P.D. Santos, Appl. Surf. Sci. 78 (1994) 57.